THE JOURNAL OF BIOLOGICAL CHEMISTRY VOL. 291, NO. 36, pp. 19068–19078, September 2, 2016

Phosphorylation of Mineralocorticoid Receptor Ligand Binding Domain Impairs Receptor Activation and Has a Dominant Negative Effect over Non-phosphorylated Receptors*

Received for publication, January 29, 2016, and in revised form, July 12, 2016 Published, JBC Papers in Press, July 15, 2016, DOI 10.1074/jbc.M116.718395

Rubén Jiménez-Canino,[1] Miguel X. Fernandes, and Diego Alvarez de la Rosa[2]

From the Departamento de Ciencias Médicas Básicas, Instituto de Tecnologías Biomédicas y Centro de Investigaciones Biomédicas de Canarias (CIBICAN), Universidad de La Laguna, 38071 La Laguna, Tenerife, Spain

Post-translational modification of steroid receptors allows fine-tuning different properties of this family of proteins, including stability, activation, or interaction with co-regulators. Recently, a novel effect of phosphorylation on steroid receptor biology was described. Phosphorylation of human mineralocorticoid receptor (MR) on Ser-843, a residue placed on the ligand binding domain, lowers affinity for agonists, producing inhibition of gene transactivation. We now show that MR inhibition by phosphorylation occurs even at high agonist concentration, suggesting that phosphorylation may also impair coupling between ligand binding and receptor activation. Our results demonstrate that agonists are able to induce partial nuclear translocation of MR but fail to produce transactivation due at least in part to impaired co-activator recruitment. The inhibitory effect of phosphorylation on MR acts in a dominant-negative manner, effectively amplifying its functional effect on gene transactivation.

Steroid receptors (SRs)[3] are part of the nuclear receptor superfamily of ligand-dependent transcription factors that modulate gene transcription in response to changes in steroid hormone levels (1). SRs present a modular architecture, with three well defined domains: an NH_2-terminal activation domain (NTD), a central DNA binding domain, and a COOH-terminal ligand binding domain (LBD). Generally, the apo receptor resides in the cytosol forming a heterocomplex with other proteins including chaperones such as heat-shock protein 90 (Hsp90). Ligand binding alters SR conformation, releasing it from the complex and promoting translocation to the nucleus, where it binds specific DNA sequences as a dimer and alters transcription of target genes by recruiting transcriptional co-regulators (2). Post-translational modifications, including phosphorylation, ubiquitylation, sumoylation, and acetylation, modulate SR stability and different steps on the activation pathway, including receptor dimerization, DNA binding, and interaction with co-regulators (3).

Until recently, it was widely assumed that SR ligand affinity is an intrinsic property defined by the structure of the LBD and not subject to modulation by post-translational modifications. However, Shibata *et al.* (4) have shown that regulated phosphorylation of Ser-843 in the LBD of human mineralocorticoid receptor (MR), a canonical member of the SR subfamily of nuclear receptors, impairs its ability to mediate gene transactivation by lowering ligand affinity. MR is closely related to the glucocorticoid receptor (GR) and can be activated under physiological conditions by mineralocorticoids such as aldosterone and glucocorticoids such as cortisol or corticosterone. MR has a wide variety of physiological and pathophysiological functions, with a prominent role in regulating transepithelial ion and fluid transport, which is essential for extracellular volume homeostasis and, therefore, blood pressure control. Phosphorylation of MR Ser-843 is restricted to intercalated cells of the distal nephron, where it has a physiological role in controlling the differential activation of MR by aldosterone under two different physiological conditions (volume depletion *versus* hyperkalemia) (4).

Working with an MR phosphomimetic mutant, Shibata *et al.* (4) showed that Ser-843 phosphorylation results in the loss of ligand-induced nuclear translocation at physiological concentrations of aldosterone (1 nM) and, consequently, a loss of gene transactivation. Ligand binding affinity is decreased by 2 orders of magnitude (K_d for [^{3}H]aldosterone changed from 0.64 nM in the wild-type receptor to 86 nM in mutant S843E) (4). Structural modeling of the LBD suggested that phosphorylation of residue Ser-843 may affect the interaction between helices H6 and H7 in the ligand-bound state.

Based on these results, we set out to answer two different but related questions. 1) Does the phosphorylation of Ser-843 result only in decreased binding affinity or does it also affect coupling between ligand binding and receptor activation? 2) How does the proportion of phosphorylated *versus* non-phosphorylated MR affect receptor function? Our results demon-

* This work was supported by Ministerio de Economía y Competitividad (Spain) Grant BFU2013-47089-R, European Cooperation on Science and Technology (COST) network ADMIRE BM1301, and the European Union Seventh Framework Program "Capacities" (FP7-REGPOT-2012-CT2012-31637-IMBRAIN). The authors declare that they have no conflicts of interest with the contents of this article.
[1] Supported by predoctoral fellowships from Cajacanarias (Spain) and Formación de Profesorado Universitario (FPU) Program (Ministerio de Educación, Spain).
[2] To whom correspondence should be addressed. Tel.: 34-922-319-968; Fax: 34-922-319-397; E-mail: diego.alvarez@ull.edu.es.
[3] The abbreviations used are: SR, steroid receptor; GR, glucocorticoid receptor; Hsp90, heat-shock protein 90; LBD, ligand-binding domain; MR, mineralocorticoid receptor; NTD, NH_2-terminal domain; PLA, proximity ligation assay; SRC-1, steroid receptor co-activator 1; YFP, yellow fluorescent protein.

strate that agonists at high concentrations are able to induce near-complete nuclear translocation of phosphomimetic mutant receptors, albeit at a much slower rate, but are ineffective in inducing agonist-dependent gene transactivation. This suggests altered coupling between ligand binding and receptor activation, resulting in impaired interaction with co-regulators. Moreover, phosphomimetic MR mutants have a dominant negative effect on WT receptor function, a feature that will amplify the physiological effect of LBD phosphorylation.

Results

This study used a previously described fluorescent derivative of mouse wild-type MR with insertion of yellow fluorescent protein (YFP) after amino acid 147 of the MR sequence (5). This construct is indistinguishable from the wild-type mouse receptor in hormone-induced nuclear translocation, apparent affinity for ligand-induced gene transactivation, DNA binding, and regulation of non-genomic pathways (5). The construct, originally named MR-YFP-147 but referred to as MR-WT in this study, was the basis to introduce phosphomimetic mutants S839D and S839E (mouse Ser-839 is the equivalent of human MR S843). To ensure that these constructs display the expected affinities for aldosterone and are comparable with those described by Shibata *et al.* (4) using human MR, we calculated equilibrium dissociation constants (K_d) with competitive binding assay in transfected COS-7 cells (Fig. 1). Results showed a K_d of 1.07 nM for fluorescent MR-WT, which is in the expected range for a wild-type receptor (K_d 0.5–2 nM; Ref. 6). Phosphomimetic mutants S839D and S839E presented decreased affinity for aldosterone, with K_d values of 86.7 and 34.3 nM, respectively, which are in the same range of the K_d value described for the equivalent mutation S843E in the human MR clone.

We then asked whether phosphorylation of MR at residue 843 impairs receptor activity exclusively by lowering ligand affinity or whether it also uncouples ligand binding from receptor activation. If the first option is correct, increasing aldosterone concentration should result in normal nuclear translocation and gene transactivation. To test this hypothesis we studied aldosterone-induced nuclear translocation using our fluorescent derivative of wild-type mouse MR (MR-WT) and compared it with the same receptor harboring phosphomimetic mutations. COS-7 cells transfected with WT, S839E, or S839D MR were left untreated or exposed overnight to increasing concentrations of aldosterone (0.1–100 nM) covering a range of physiological (0.1–2 nM) to supra-physiological levels. In the absence of ligand the vast majority of cells showed a predominantly cytosolic MR localization (Fig. 2, *A* and *C*) as previously described (7, 8). Mutations S839D or S839E did not change naïve MR subcellular localization (Fig. 2, *A* and *C*). When cells were stimulated overnight with increasing concentrations of aldosterone, MR-WT translocated to the nucleus, with >90% of the cells showing an exclusive MR nuclear localization with as little as 1 nM aldosterone (Fig. 2, *A* and *C*). In comparison, aldosterone partially translocated mutants MR-S839D and MR-S839E. The effect started to be apparent at 1 nM aldosterone and continued growing with up to 100 nM aldosterone, where ~90% of cells showed a predominantly nuclear localization (Fig. 2, *B* and *C*). These results suggests that phosphorylation of MR impairs nuclear translocation but only to a limited extent, with a significant amount of receptor present in the nucleus.

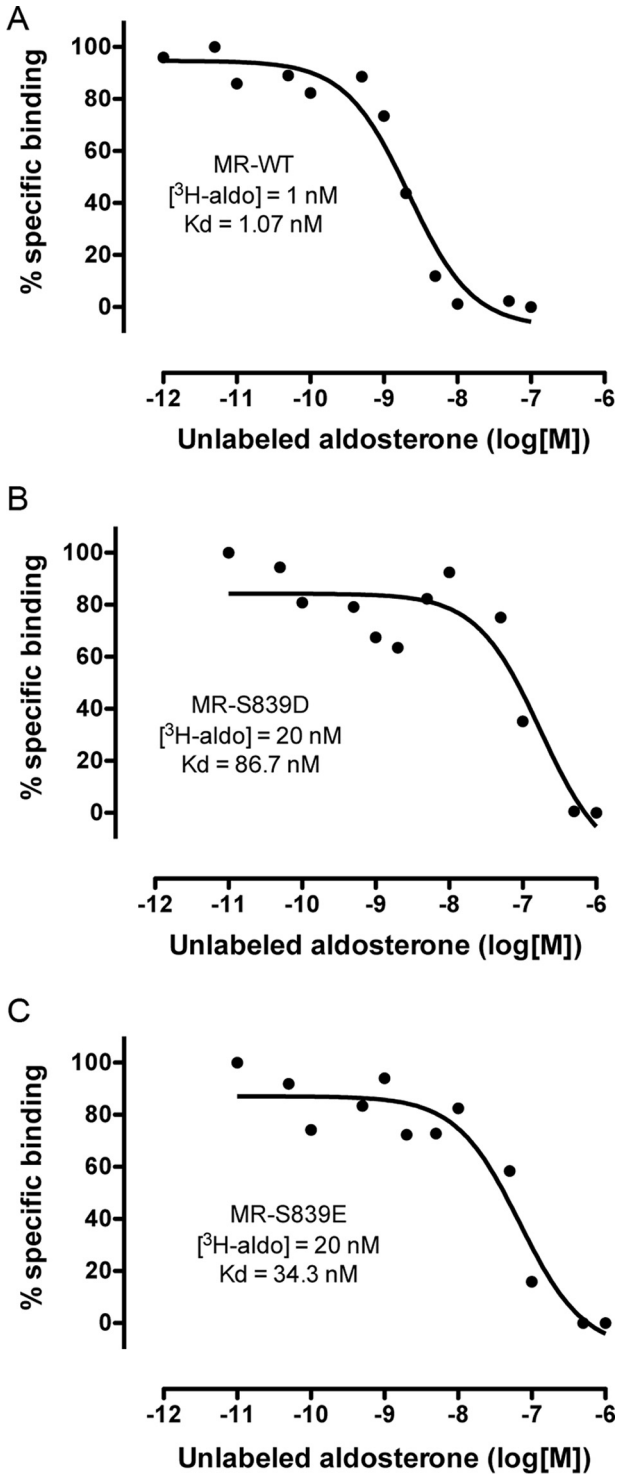

FIGURE 1. **Phosphomimicking mutants MR-S839D and MR-S829E show decreased affinity for aldosterone.** COS-7 cells were transfected with WT or mutant MR and the binding affinity for [^{3}H]aldosterone (*aldo*) was measured using a competitive binding assay. Cells were treated with a fixed concentration of [^{3}H]aldosterone (1 nM for WT and 20 nM for mutant MR) in the presence of increasing concentrations of unlabeled aldosterone. *A*, wild-type MR (MR-WT). *B*, MR mutant S839D (MR-S839D). *C*, MR mutant S839E (MR-S839E). Data points are an average of duplicate measurements and represent normalized specific binding. Calculated K_d values are indicated for each plot.

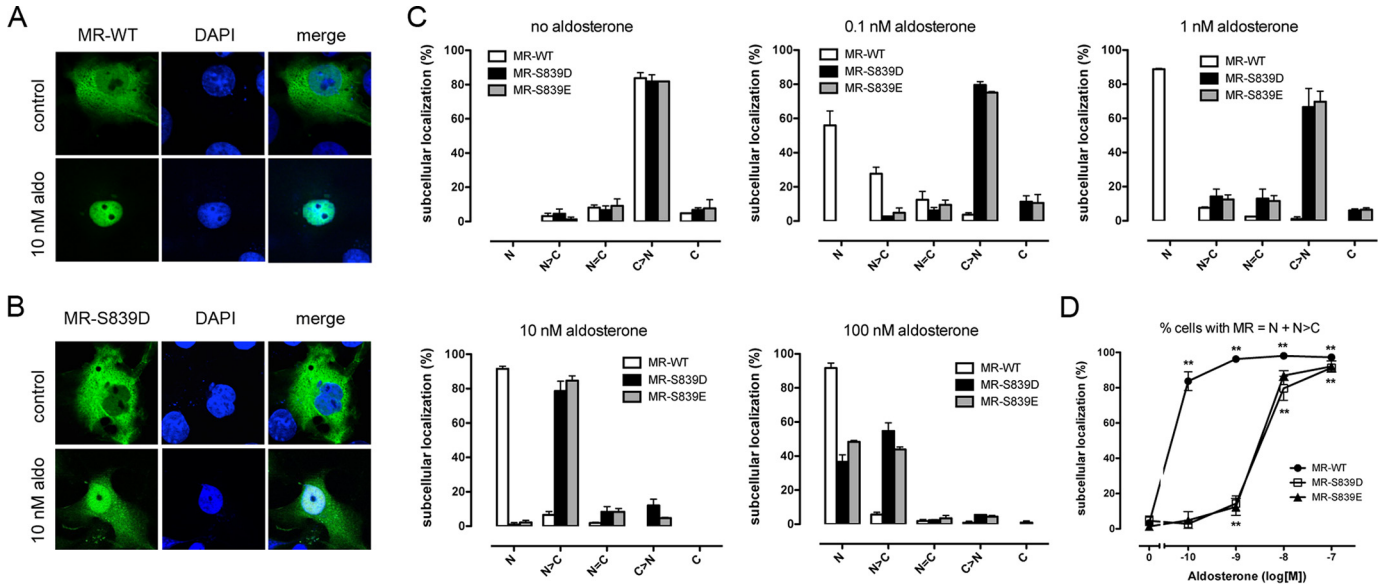

FIGURE 2. **Phosphomimetic mutants MR-S839D and MR-S839E show partial ligand-induced nuclear translocation.** *A*, representative images of YFP-tagged wild-type MR (*WT*) subcellular localization in COS-7 cells in the absence of ligand or after overnight treatment with 10 nM aldosterone. *B*, representative images of YFP-tagged MR-S839D subcellular localization in COS-7 cells in the absence of ligand or after overnight treatment with 10 nM aldosterone. *C*, quantitative analysis of MR-WT, MR-S839D, and MR-S839E subcellular localization in the absence of ligand or after 16 h stimulation with the indicated concentrations of aldosterone. Cells were scored into five different categories reflecting the localization of MR (*C*, exclusively cytosolic; $C > N$ predominantly cytosolic; $C = N$ evenly distributed between nucleus and cytosol; $C < N$, predominantly nuclear; *N*, exclusively nuclear). *Bars* represent the average percentage of cells ± S.E. scored under each category ($n = 3$ independent experiment, with at least 75 cells scored in each group and experiment). No significant differences between mutants S839D and S839E were detected in any of the conditions tested (unpaired *t* test). *D*, plot summarizing data shown in *panel C*; each point represents the % of cells with either predominantly nuclear ($C < N$) or exclusively nuclear (*N*) MR localization for each of the three constructs (*WT*, *S839D*, and *S839E*). Note that the *x* axis has been split in two segments to be able to represent data from untreated (no aldosterone) cells next to the treated cells in a log scale. **, $p < 0.01$ compared with control (no aldosterone) condition, one-way analysis of variance, followed by Dunnett's multiple comparison test.

To test whether decreased nuclear localization induced by phosphorylation arises from slower nuclear import, we examined the kinetics of this process in COS-7 cells transfected with MR-WT or phosphomimetic mutation S839D (both tagged with YFP). To that end, living cells were placed under a confocal microscope in a temperature-controlled chamber at 37 °C and stimulated with 10 nM aldosterone. Images of the same cells were taken every 2 min for up to 60 min after the addition of the hormone, and the proportion of nuclear receptor was calculated in every cell for each time point. Representative images of WT and S839D MR translocation are shown in Fig. 3*A*. When compared with the WT receptor, mutant S839D showed very slow translocation kinetics, with <20% of the cytosolic receptor translocated over the period of 1 h (Fig. 3, *A* and *B*). This strongly suggests that impaired ligand-induced nuclear accumulation of the phosphomimetic MR mutant arises from slower nuclear import. This in turn may arise from lower affinity for the ligand but could also imply either decreased stability of aldosterone in the LBD or a defect in coupling ligand binding with receptor conformational change.

We then tested the functional consequences of mutating mouse MR residue Ser-839 for MR-mediated gene transactivation. We tested non-phosphorylatable mutant S839A and phosphomimicking mutants S839D and S839E. Aldosterone dose-response luciferase reporter assays showed an EC_{50} of 0.4 nM for MR WT, whereas S839A EC_{50} was 2.8 nM. Upon stimulation with cortisol, WT MR displayed an EC_{50} of 9.8 nM, and MR-S839A had an EC_{50} of 19.3. As described with human MR-S843E, mouse MR-S839E and mouse MR-S839D did not

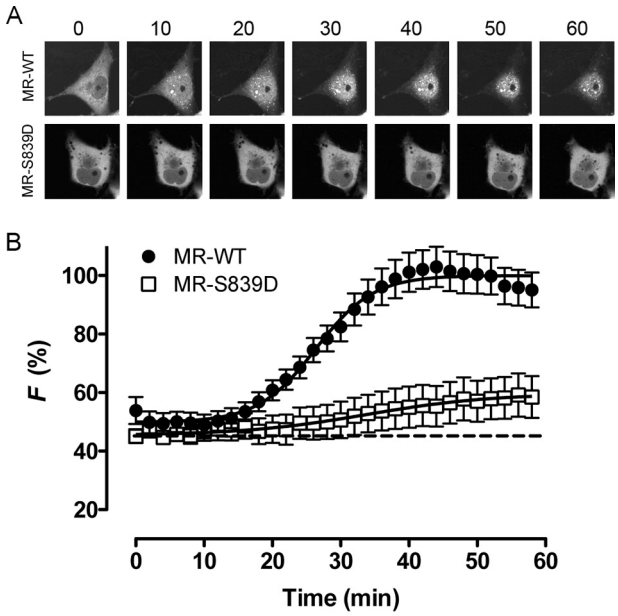

FIGURE 3. **MR-S839D shows a drastically reduced ligand-induced nuclear translocation rate.** *A*, representative images of cells transfected with YFP-tagged wild-type MR (*MR-WT*) or mutant S839D (*MR-S839D*) and examined under confocal microscopy at 37 °C to detect nuclear translocation induced by 10 nM aldosterone. *Numbers* refer to time after the addition of aldosterone (min). *B*, quantitative analysis of MR-WT or MR-S839D nuclear translocation. Individual points represent average ± S.E. ($n = 9$) percentage nuclear fluorescence intensity *versus* total cellular fluorescence (*F*). Images taken once every 2 min after the addition of 10 nM aldosterone, up to 60 min. Data points were fitted to Boltzmann sigmoid curves. The *dashed line* indicates the basal level of percentage nuclear localization.

display aldosterone or cortisol-dependent gene transactivation even at high doses of ligand (Fig. 4, *A* and *B*). Western blotting analysis showed that the lack of MR-S839D or MR-S839E transactivation and reduced MR-S839A transactivation were not due to impaired protein expression (Fig. 4*C*).

The lack of any gene transactivation by MR-S839E or MR-S839D at ligand concentrations where there is significant nuclear translocation in the same time frame (compare Fig. 2 and Fig. 4) supports the idea that phosphorylation of MR LBD not only lowers MR affinity for agonists but has a profound impact on the ability of the ligand to activate the receptor. Therefore, we hypothesized that the phosphomimetic mutant may prevent efficient interaction with co-regulators. To investigate this possibility we tested ligand-induced MR interaction with a well known co-activator, steroid receptor co-activator 1 (SRC-1) (9–11). SRC-1 displays a predominantly nuclear localization both in control and aldosterone-stimulated conditions, whereas MR shows the expected ligand-induced trafficking from cytosol to nucleus (Fig. 5*A*). To quantitatively assess MR-SRC-1 interaction, we used a proximity ligation assay (PLA). Co-transfection of MR-WT and SRC-1 resulted in a prominent PLA signal in the cell nucleus only in the presence of aldosterone (Fig. 5*B*). Omission of either one of the transfected plasmids resulted in the absence of signal (Fig. 5, *B* and *C*). Quantitative analysis demonstrated that PLA signal was drastically reduced (to ~15% of the WT signal) when the phosphomimetic mutants MR-S839D or MR-S839E were co-transfected with SRC-1 (Fig. 5, *B* and *C*).

Based on MR LBD crystal structure, Shibata *et al.* (4) predicted that phosphorylation of residue Ser-843 could affect ligand binding and/or receptor activation. Indeed, their experimental measurements of WT and phosphomimetic mutant S843E K_d for aldosterone showed decreased affinity (from 0.63 nM to 86 nM) (4). To further investigate the possible effects of phosphorylation at Ser-843, we modeled this post-translational modification using available crystal structures of MR LBD as templates (12). Using this model we performed docking calculations to estimate the energy of interaction of aldosterone, cortisol, and spironolactone to MR LBD in the WT form with phosphorylated Ser-843 or introducing phosphomimetic mutation S843D (Table 1). To validate docking parameterization, we compared the position of aldosterone as calculated by docking with the position of aldosterone as determined by x-ray crystallography. Both were practically superimposable (not shown). Docking interaction energy for aldosterone was only slightly affected by phospho-Ser-843, S843D or S839E modifications (Table 1), suggesting that the decreased affinity observed by Shibata *et al.* (4) may have a kinetic basis rather than a change in equilibrium interaction. Given that intercalated cells, where Ser-843 phosphorylation has been described, lack 11-β-hydroxysteroid-dehydrogenase type 2 and its MR may, therefore, be activated by cortisol (4, 13), we also calculated docking energy for this hormone. In contrast to aldosterone, cortisol appears to bind slightly more stably to the modified LBD (Table 1), again suggesting that the absence of cortisol transactivation of phosphomimetic mutants observed previously (4) and confirmed here (Fig. 4*B*) does not arise from impaired equilibrium interaction with MR LBD. Spironolac-

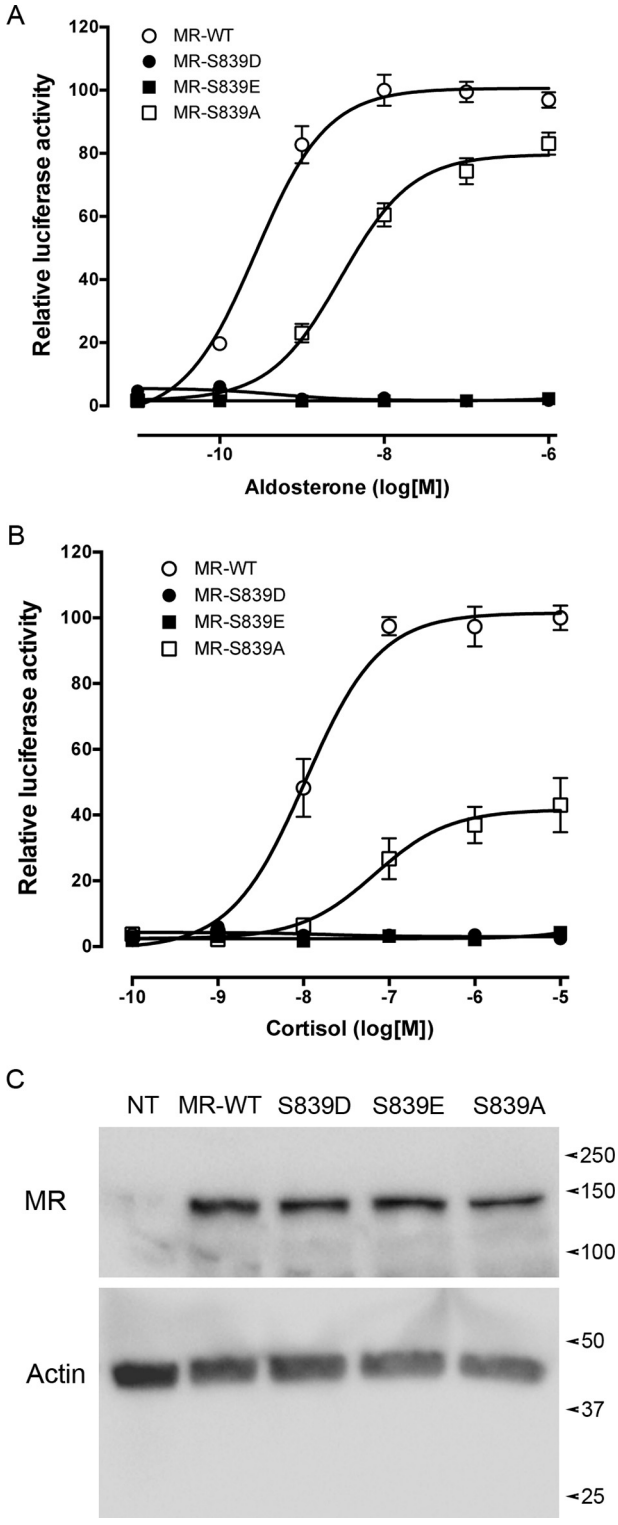

FIGURE 4. **MR-S839D and MR-S839E mutants are unable to mediate ligand-induced gene transactivation.** Aldosterone (*A*) and cortisol (*B*) dose-response gene transactivation curves corresponding to WT MR, or mutants MR-S843D, MR-S839E, and MR-S843A. Individual points represent the average ± S.E. ($n = 3$) firefly/*Renilla* values normalized to the maximum activity in each construct. Data points were fitted to a variable slope model (four parameters). *C*, Western blotting analysis of WT and mutant MR expression in COS-7 cells. *NT*, non transfected cells. The same blot was consecutively probed with anti-MR and anti-β-actin antibodies. *Arrowheads* mark the migration of molecular mass markers (values in kDa).

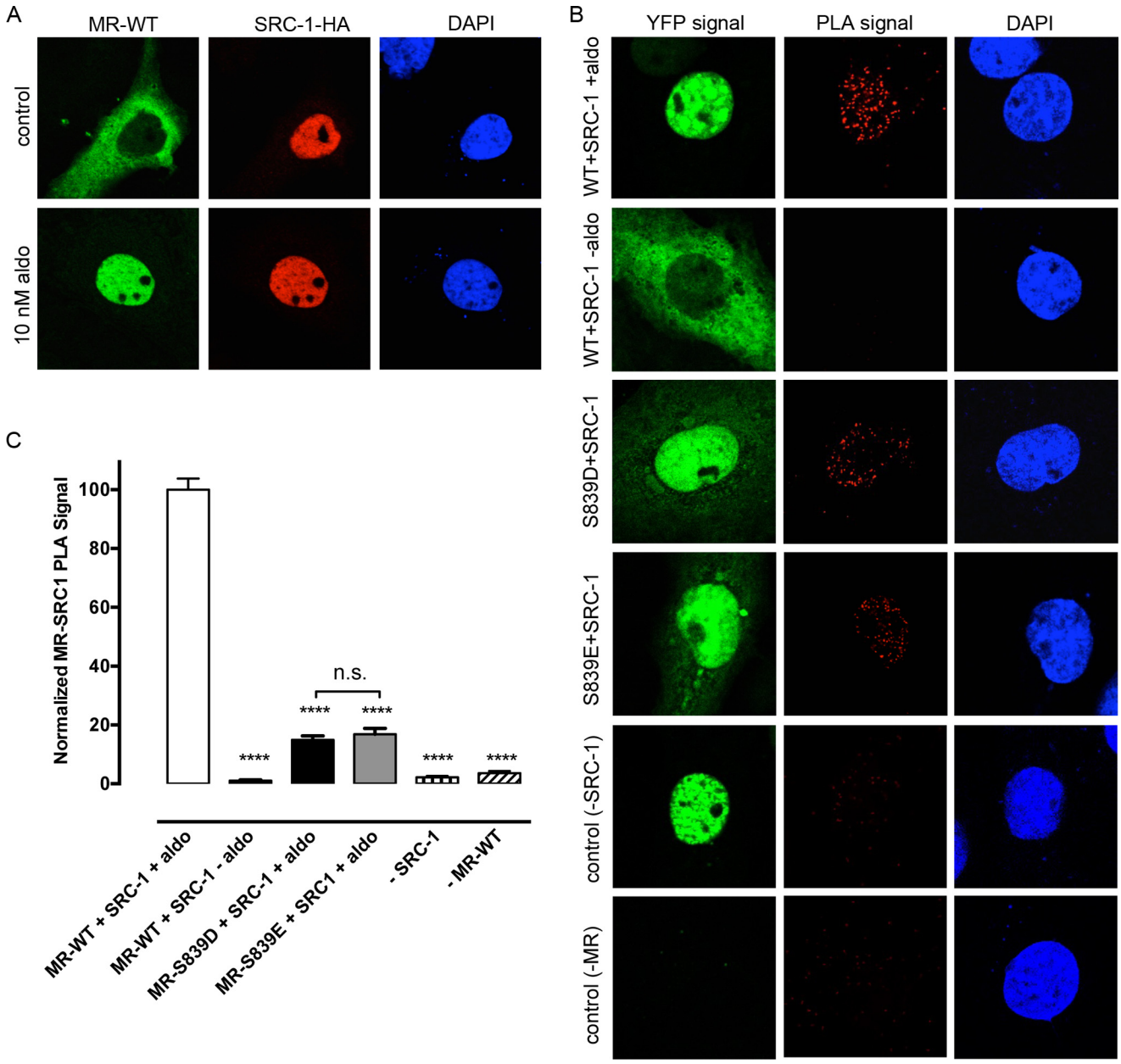

FIGURE 5. **Phosphomimetic mutants MR-S839D and MR-S839E impair interaction with co-activator SRC-1 after aldosterone treatment.** *A*, subcellular distribution of YFP-tagged wild-type MR (*MR-WT*) and HA-tagged SRC-1 transfected in COS-7 cells and treated or not with 10 nM aldosterone (*aldo*) for 24 h. *B*, representative images of proximity ligation assay results examining the interaction of MR with SRC-1. *C*, quantitative analysis of MR-SRC-1 interaction when WT or mutant MR were co-transfected with SCR-1 and treated with 10 nM aldosterone. *Bars* represent the average number of puncta/cell ± S.E. ($n = 36–40$ cells per condition). Negative controls consisted on the omission of aldosterone treatment (−*aldo*) or leaving out either MR (−*MR-WT*) or SRC-1 (−*SRC-1*) from the transfection mix. ****, $p < 0.0001$; *n.s.*, no significant difference when compared with MR-WT+aldo condition; Kruskal-Wallis test followed by Dunn's multiple comparisons test.

TABLE 1

Docking interaction energies (kcal mol^{-1}) of ligands with modeled MR WT, mutant, or phosphorylated ligand binding domain

Calculations assume an error of ± 0.3 kcal mol^{-1}.

MR LBD variant	Aldosterone	Cortisol	Spironolactone
Ser-843	−11.3	−9.9	−13.2
S843D	−10.8	−10.8	−12.2
S843E	−11.3	−11.2	−13.5
Ser(P)-843	−10.8	−10.6	−12.3

tone showed a decrease in docking energy interaction with Ser-843 phosphorylation and S843D mutation but not with S843E mutation (Table 1). Interestingly, interaction energies for the three ligands were almost identical in the model incorporating a phosphorylation of Ser-843 when compared with mutation S843D (Table 1) but not compared with mutation S843E, suggesting that using phosphomimetic mutation S843D may be a better approximation to study the effects of Ser-843 phosphorylation in MR function.

To investigate the functional impact of partial MR phosphorylation we co-expressed different proportions of WT and S843D receptors in COS-7 cells. To ensure that the different proportions of plasmids produced the desired protein expression levels, we performed Western blotting analysis of receptor expression. Both receptors were recognized by the same

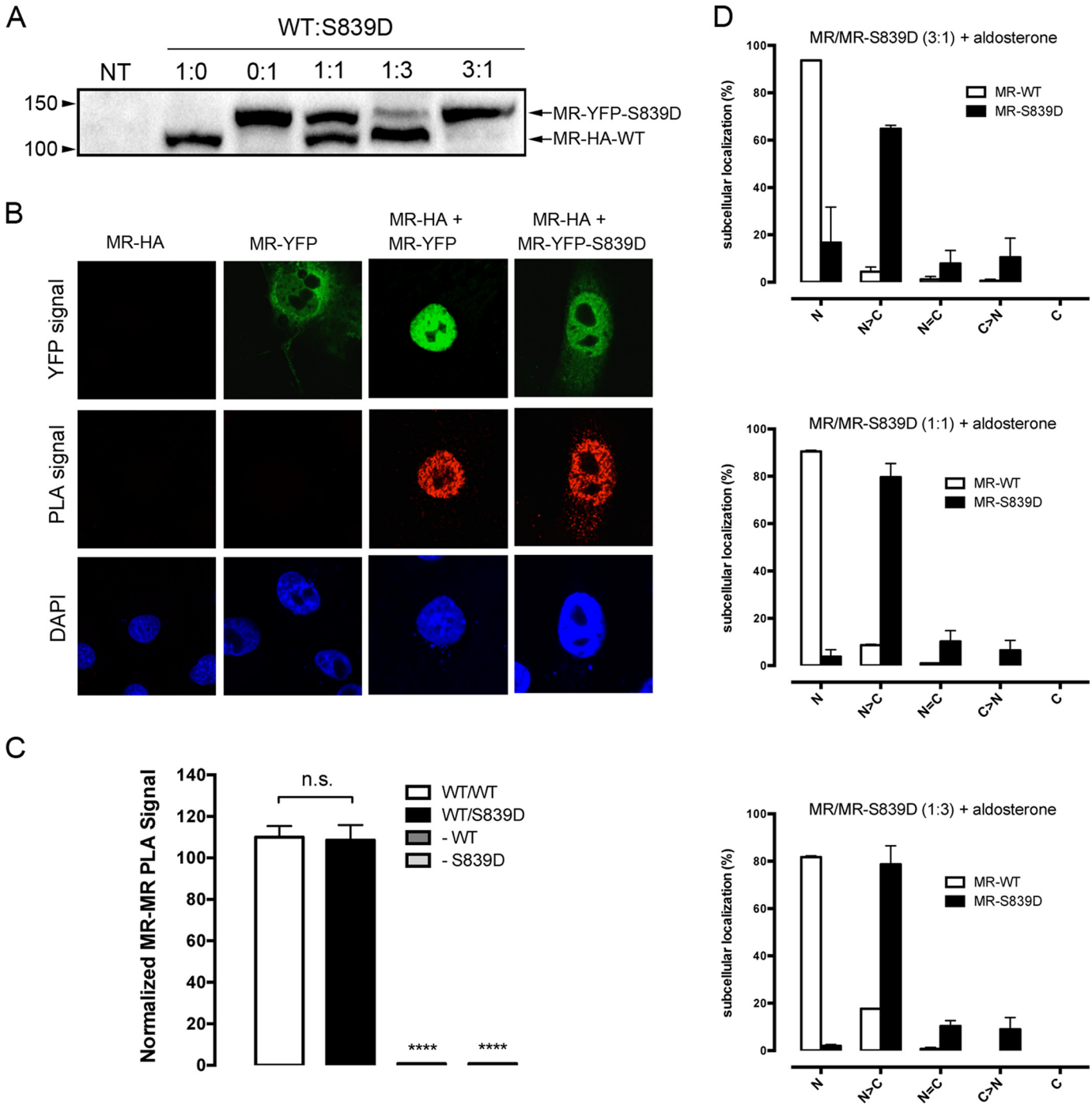

FIGURE 6. **MR-WT and MR-S839D dimerize normally and show partial nuclear translocation.** *A*, Western blotting analysis of HA-tagged wild-type MR (*MR-HA-WT*) and YFP-tagged MR S839D mutant (*MR-YFP-S839D*) protein levels after transfection of coding plasmid in the indicated proportions (WT·S839D). *NT*, non transfected cells. To differentiate between WT and mutant proteins a construct containing YFP and mutation S839D was used. *Arrowheads* indicate the migration of molecular mass markers (values in KDa). *B*, representative images of proximity ligation assays showing equal level of MR dimerization in the absence or presence of S839D mutation. *C*, quantitative analysis of of MR-HA-WT interaction when MR-YFP-WT or mutant MR-YFP-S839D in cells treated with 10 nM aldosterone. Negative controls consisted on the omission of either the MR-HA-WT (−*WT*) or the MR-YFP-S839D (−*S839D*) plasmids in the co-transfection. *Bars* represent the average number of puncta/cell ± S.E. ($n = 35–45$ cells per condition; *n.s.*, no significant difference; ****, $p < 0.0001$; Student's *t* test). *D*, quantitative analysis of wild-type and S839D MR subcellular localization co-expressed in different proportions (3:1; 1:1, or 1:3) and stimulated with 10 nM aldosterone for 16 h.

anti-MR antibody but could be differentiated due to their different molecular weight produced by fusing YFP to MR-S839D. Co-expression of both receptors using 1:3, 1:1, and 3:1 plasmid proportions gave the expected ratios between WT and mutant MR (Fig. 6*A*). To confirm that S843D mutation does not disrupt dimerization and it is able to form dimers with WT MR, we used PLA (Fig. 6*B*). Quantification of PLA results showed that MR dimerization was identical in the absence or presence of the S839D mutation (Fig. 6*C*). This result indicates that WT MR subunits do not discriminate between WT and S839D-contain-

TABLE 2

Expected subunit composition of wild type and S839D heterodimers

Probabilities of different dimers are shown below for each possible plasmid combination, expressed in percentage. Assuming that both plasmids are processed equally to produce protein and that dimerization is not affected by S839D mutation, it is expected that the probability of heterodimer composition follows a binomial distribution given by the expression $p_i = P_{wt}^{i} P_m^{n-i}$, where p_i is the probability of i (0, 1, or 2) wild type subunits in a dimer ($n = 2$), and P_{wt} and P_m are the probabilities of encountering a wild type or S839D mutant in the total protein pool depending on the proportions of plasmids transfected.

Transfected proportions	Type of dimer formed		
	WT·WT	WT·S839D	S839D·S839D
3:1	56.25%	37.5%	6.25%
1:1	25	50	25
1:3	6.25%	37.5%	56.25%

ing subunits for dimerization. Therefore, we predicted that the distribution of WT·WT, WT·S839D, and S839D·S839D dimers when different proportions of WT MR and S839D mutant are co-transfected should follow a binomial distribution (calculated abundances of each type of dimer are shown in Table 2). We next investigated subcellular localization of three different conditions where WT·S839D proportions were variable (Fig. 6*D*). Subcellular distribution in the absence of ligand did not show any variation, as predicted by experiments transfecting each variant individually (shown in Fig. 1*B*). Subcellular localization of WT and S839D proteins in the presence of 10 nM aldosterone varied consistently with partially impaired nuclear localization of the S839D mutant (Fig. 6*D* and Table 3). Transactivation levels corresponded closely with the predicted amounts of WT homodimers (Fig. 7 and Table 2), indicating that heterodimers between WT and phosphomimetic S839D MR are transcriptionally inactive (Fig. 7). These results demonstrate that phosphorylation at residue Ser-839 has a dominant negative effect on MR activity.

It has previously been described that MR is able to heterodimerize with GR and affect its function. Using COS-7 cells as an expression model, Liu *et al.* (14) demonstrated that co-expression of MR diminishes GR-dependent transactivation, likely due to weak transcriptional activity of heterodimers. To test whether phosphorylation of MR residue Ser-839 affects GR activity, we co-transfected COS-7 cells with GR, WT MR, or phosphomimicking mutant MR-S839D and assessed dose dependence of cortisol-induced transactivation. MR and GR co-expression at a 1:1 ratio decreased luciferase induction by 50% at saturating cortisol concentrations when compared with GR expressed alone (Fig. 8*A*), consistent with previously published data (14). When GR was co-expressed with MR-S839D at a 1:1 ratio luciferase, transactivation further decreased to 25% that of maximum activity achieved when GR was expressed alone (Fig. 8*A*). The effect of MR-S839D co-expression on cortisol-induced MR activity was the same as the one detected with aldosterone (Fig. 8*B*). These observations are consistent with a model where MR·GR heterodimers possess very low or null transactivation capacity, with most of the detected cortisol-induced transactivation being conducted by GR·GR and MR·MR heterodimers. Because phosphorylated MR is inactive and acts as dominant negative toward non-phosphorylated MR, this post-translational modification would only further decrease cortisol-mediated gene transactivation in cells co-expressing MR and GR.

TABLE 3

Subcellular localization of MR and MR-S839D co-expressed in COS-7 cells at different proportions and stimulated with 10 nM aldosterone for 16 h

Values express average percentage of cells in each category as obtained in the experiments shown in Fig. 6*C*. Rows corresponding to unmixed conditions (only one plasmid transfected) contain dashes to indicate the missing MR form (WT or S839D mutant).

MR·MR-S839D[a]	N		N > C		N + N > C[b]	
	WT	S839D	WT	S839D	WT	S839D
1:0	91.5	–	6.6	–	98.1	–
0:1	–	1.0	–	78.6	–	79.6
3:1	93.7	16.7	4.4	64.8	98.1	81.5
1:1	90.4	3.8	8.6	79.6	99.1	83.4
1:3	81.7	1.9	17.6	78.7	99.3	80.6

[a] Proportions of transfected plasmids.
[b] Values obtained by adding the percentage of cells in N and N>C categories.

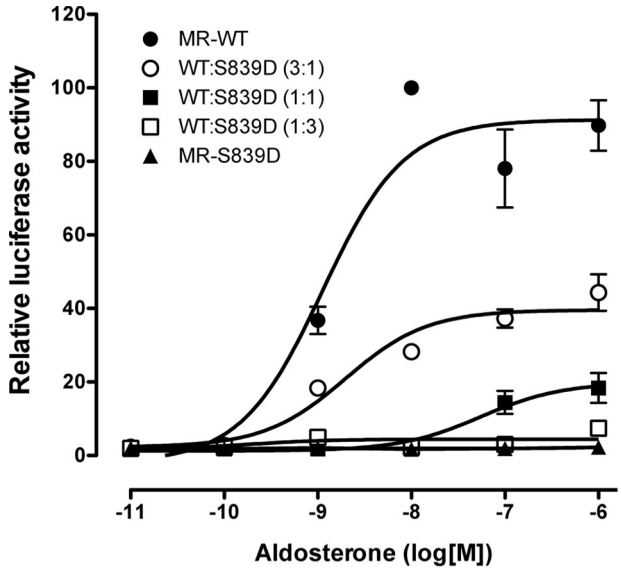

FIGURE 7. **Phosphomimetic mutant MR-S839D displays dominant-negative activity over wild-type MR.** The plot represents aldosterone-dependent reporter transactivation obtained after co-expression of wild-type and S839D MR in the indicated proportions. Individual points represent the average ± S.E. ($n = 3$) firefly/*Renilla* values normalized to the maximum activity in each construct. Data points were fitted to a variable slope model (four parameters).

Discussion

Our results show that physiological and supra-physiological doses of aldosterone are able to induce at least partial translocation of phosphomimetic mutants MR-S839D and S839E, but the mutants are totally impaired for gene transactivation. This correlates with an inability to recruit a common MR co-activator, SRC-1. *In silico* modeling of the effect of Ser-839 phosphorylation on ligand docking energy suggests that this modification displays minor effects on steady-state ligand interaction. When co-expressed with WT receptor, MR-S839D decreased gene transactivation to an extent consistent with a dominant negative role in the SR dimer, consistent with a model where only one phosphorylated unit in the dimer will completely impair MR activity. Finally, our data suggest that MR phosphorylation at residue S839D will further impact cortisol-induced gene transactivation in cells co-expressing MR and GR.

Based on the previous work by Shibata *et al.* (4) and the data presented in this work, we can clearly see how there is good agreement between WT receptor K_d (1.07 nM) and EC_{50} (0.4 nM) for aldosterone. In contrast, there is a large difference when

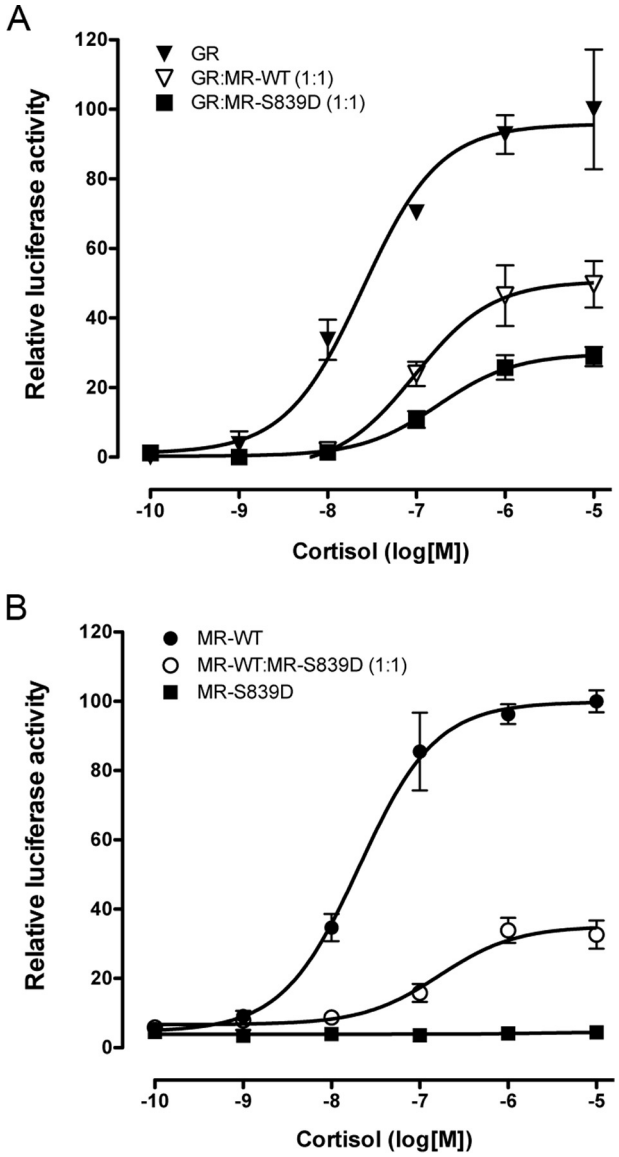

FIGURE 8. **Expression of phosphomimetic mutant MR-S839D lowers cortisol-induced gene transactivation when MR and GR are co-expressed in the same cell.** *A*, Cortisol-dependent reporter transactivation obtained after co-expression of wild-type or S839D MR with wild-type GR in the indicated proportions. *B*, Cortisol-dependent reporter transactivation obtained with wild-type MR, MR-S839D, or after co-expression of wild-type and mutant receptors. Individual points represent the average ± S.E. ($n = 3$) firefly/*Renilla* values normalized to the maximum activity. Data points were fitted to a variable slope model (four parameters).

phosphomimetic mutants S839D or S839E (Ser-843 in the human sequence) are examined, with a K_d of 86.7 and 34.3 nM, respectively, but no gene transactivation detectable, even at 1 μM aldosterone (see Fig. 4*A*). This discrepancy between K_d and EC_{50} is reminiscent of MR activation by cortisol. K_d for cortisol and aldosterone are in the same order of magnitude (0.5–2 nM), but EC_{50} for cortisol is 10 nM (for review see Ref. 6). The discrepancy between K_d and EC_{50} for cortisol-induced MR activation has been explained by the fast off-rate of cortisol from the complex (15–17). If this applies to the case of MR-Ser-839 phosphorylation, then one would expect to see a decreased nuclear translocation rate along with decreased apparent affinity for aldosterone-induced transactivation. Shibata *et al.* (4) found no aldosterone-induced translocation of the phosphomimetic mutant, but they used a physiological dose of 1 nM aldosterone. In our experiments we could demonstrate partial translocation of the mutant receptor, with an increasing proportion of nuclear receptor following a dose-response relationship with aldosterone concentration (Fig. 2*D*). Surprisingly, no transactivation was detected, even at a high dose of aldosterone. Kino *et al.* (18) found that cyclin-dependent kinase 5-mediated neuronal MR phosphorylation at residues Ser-128, Ser-250, and Thr-159 (all placed in the NTD) dramatically interferes with MR activity but not with ligand-dependent nuclear accumulation. The authors interpreted this effect as a phosphorylation-dependent block of co-regulator interaction with the NTD without affecting hormone binding and receptor transformation associated to translocation. In the case of MR phosphorylation at Ser-839, it appears that, in addition to reduced agonist affinity, ligand binding-induced conformational changes are sufficient for nuclear translocation (even though it is performed at a much lower rate). However, ligand binding is clearly unable to support appropriate co-activator recruitment and gene transactivation, suggesting that the conformational change is either incorrect or unstable. This idea is further supported by recent work by Mani *et al.* (19) showing that mutation of human MR residue Ser-843 to proline (the amino acid present in the equivalent position in GR) does not affect MR affinity for aldosterone or cortisol but dramatically increases gene transactivation EC_{50}, suggesting an important role for this residue on receptor activation.

The above model is supported by our *in silico* analysis. Docking calculations of steady-state energy of interaction show that ligand binding is not greatly altered (in the case of cortisol, it is even more stable with the phosphorylated LBD), although an additional effect on ligand access to the binding pocket cannot be excluded. The fact that agonist binding was able to induce nuclear translocation suggests that MR LBD phosphorylation at residue Ser-839 may alter LBD conformational dynamics so that LBD-co-regulator protein-protein interaction interphase is altered (11, 16, 20).

The lack of transactivation function in mutants S839D and S839E made us wonder what would be the functional consequence of dimer formation between WT and phosphomimetic mutant receptors. Shibata *et al.* (4) showed that cells co-expressing wild-type MR and MR-S843E and treated with 1 nM aldosterone for 1 h display full wild-type MR translocation and no MR-S843E translocation. Therefore, the authors proposed that loss of aldosterone binding and lack of subsequent nuclear translocation produces the loss of gene transactivation. However, to explain the nuclear translocation data, one must assume that WT MR and MR-S843E do not dimerize and, therefore, act independently of one another. We examined this question in detail by co-transfecting MR WT and S839D mutant. Western blotting and PLA data (Fig. 6) demonstrate that both receptors were expressed in the expected proportions and, most importantly, that they appeared to dimerize freely. This is not surprising as the main determinant of receptor dimerization is the DNA binding domain, not the LBD (14). Under these conditions, the effect of S839D on aldosterone-induced MR activity fitted perfectly with a model where only

WT·WT dimers are active, strongly suggesting that heterodimers of phosphorylated and non-phosphorylated MR would be functionally inactive. This may be explained by both units in the dimer adopting a productive conformation to be able to simultaneously recruit co-regulators. Given that MR-S839D shows impaired interaction with co-activator SRC-1, it could be the case that asymmetrical recruitment of co-activators by only one unit in the dimer (the WT one) is not sufficient to promote gene transactivation. A very important consequence of this fact is that at physiological levels of circulating aldosterone, which are in the low nM range, 50% of phosphorylated receptor would totally prevent aldosterone-dependent gene transactivation (see Fig. 6*D*). In addition, the effect of MR on decreasing GR activity (14) combined with MR phosphorylation at residue Ser-839 would imply a highly reduced cortisol-mediated gene transactivation in cells that co-express MR and GR.

In summary, we have shown that inactivation of an SR by phosphorylation in the LBD most likely arises from an uncoupling between ligand binding and receptor conformational changes, partially impairing nuclear translocation but mainly interfering with co-activator recruiting. The physiological effect of this post-translational modification will likely be amplified by the fact that it acts in a dominant-negative fashion when modified and unmodified receptors dimerize.

Experimental Procedures

Plasmid Constructs

Generation and use of a functional fluorescent derivative of MR with insertion of YFP after amino acid 147 has been previously described (5, 21). A derivative of that construct substituting YFP by three copies of the HA epitope was generated by using AscI sites flanking the YFP sequence and cloning a PCR-generated 3×HA epitope with the same flanking sites. Mouse MR phosphomimetic mutations S839D and S839E and non-phosphorylatable mutation S839A (mouse MR Ser-839 is the equivalent residue to human Ser-843) were generated using the QuikChange Lightning site-directed mutagenesis kit (Agilent) following the manufacturer's instructions. Plasmid expressing wild-type GR cloned in pcDNA3 (Invitrogen) has been described previously (15) and was a kind gift from Dr. Nicolette Farman (Centre de Recherche des Cordeliers, Paris). Plasmid pcDNA3.1-SRC-1-HA, expressing SRC-1 tagged with an HA epitope, was produced by amplifying SRC-1 by PCR from mouse hippocampus cDNA using a proofreading DNA polymerase and a reverse oligonucleotide containing the coding sequence of the HA tag followed by cloning into pcDNA3.1/V5-His-TOPO vector (pcDNA3.1 Directional TOPO® Expression kit, Thermo Fischer Scientific). All constructs and mutations were corroborated by DNA sequencing.

Cell Culture, Transfection, and Hormone Treatments

To study MR cellular dynamics and transactivation function we used COS-7 cells, which lack endogenous MR and GR expression (22). COS-7 cells were obtained from American Type Culture Collection (Manassas, VA) and maintained in DMEM supplemented with 10% FBS. Cells were transfected with Jetprime (Polyplus Transfection, Illkirch, France) following the manufacturer's instructions. When indicated, cells were washed twice with DMEM medium and then transferred to medium supplemented with charcoal-stripped serum (Lonza, Barcelona, Spain) 24 h before the experiment started. Aldosterone and cortisol were obtained from Sigma, dissolved in ethanol, and added to cells to the final concentration indicated for each experiment. Control cells were treated with ethanol at the same dilution used for treatments (1:1000).

Western Blotting Analysis

MR protein expression was analyzed by Western blotting as previously described (7). Anti-MR 1D5 monoclonal antibody developed by Gomez-Sanchez *et al.* (23) was obtained from the Developmental Studies Hybridoma Bank, created by the NICHD, National Institutes of Health and maintained at The University of Iowa Department of Biology. Rabbit polyclonal anti-GFP antibody was the kind gift of Dr. Raimundo Freire (Hospital Universitario de Canarias, Spain) and has been previously described (24). HA-tagged proteins were detected using a commercially available monoclonal antibody (clone HA.11, Covance, catalogue number MMS-101R, Madrid, Spain). Anti-mouse or anti-rabbit peroxidase conjugates (GE Healthcare) were used at 1:10,000 dilution. Western blots were developed with Immun-Star WesternC kit (Bio-Rad), and signals were detected with a Chemidoc imaging system (Bio-Rad).

Competitive Binding Assay

Receptor binding affinity for aldosterone was determined in intact cells using a competitive binding assay essentially as described (19). Briefly, transfected cells were incubated for 1 h in serum-free medium and then treated with [^{3}H]aldosterone (PerkinElmer Life Sciences; 1 nM for wild-type MR or 20 nM for S839D and S839E mutants) for 2 h at 37 °C in the presence of increasing concentrations of unlabeled aldosterone. Bound aldosterone was extracted with 80% ethanol, and radioactivity was measured by liquid scintillation. Specific binding was calculated by subtracting disintegrations per minute (dpm) obtained in the presence of 10 μM unlabeled aldosterone. Half-maximal inhibitory concentrations (IC_{50}) were calculated using nonlinear regression using Prism 5 (GraphPad, San Diego, CA). Equilibrium dissociation constants (K_d) were then calculated from the IC_{50} using the Cheng-Prussoff equation (25) in Prism 5 and assuming that labeled and unlabeled aldosterone have identical affinities so that K_d and the inhibition constant (K_i) are the same.

Analysis of MR Subcellular Localization and Nuclear Translocation Dynamics

Semiquantitative analysis of subcellular distribution in the absence of aldosterone was performed as previously described (7, 8, 26). Briefly, cells were fixed, images were taken under a confocal microscope, and at least 75 cells per condition were scored into five categories (N, exclusive nuclear localization; N > C, predominant nuclear localization; N = C, even distribution throughout cytosol and nucleus; N < C, predominant cytosolic localization; C, exclusive cytosolic localization). Data are shown as the percentage of cells in each category from the total amount of cells scored. To detect MR-3×HA, cells were immunostained following previously published procedures (26) using a monoclonal antibody against the HA epitope (clone

HA.11, Covance) and goat anti-mouse secondary antibodies conjugated to Alexa fluor 594 (Invitrogen). Images were collected using a Fluoview 1000 confocal microscope (Olympus, Barcelona, Spain). Kinetic analysis of aldosterone-induced MR nuclear translocation was performed as previously described (21, 26). Briefly, cells were transfected with MR-YFP and grown for 48 h in DMEM supplemented with charcoal-stripped FBS. Cells were then transferred to extracellular saline (137 mM NaCl, 4 mM KCl, 1.8 mM $CaCl_2$, 1 mM $MgCl_2$, 10 mM glucose, 10 mM HEPES, pH 7.4), placed under the confocal microscope in a temperature-controlled environmental chamber set at 37 °C, and treated by adding 10 nM aldosterone to the medium. Images were collected at a sampling rate of 1 every 2 min for 1 h. Quantitative analysis of MR-YFP distribution was performed frame-by-frame using the manufacturer's software (Olympus). Controls in the absence of aldosterone were performed to control for photobleaching of YFP. Data processing and sigmoid curve-fitting were performed using Prism 5 (GraphPad) according to Equation 1:

$$F = F_0 + \left[\frac{F_{max} - F_0}{1 + \exp\left(\frac{t_{1/2} - t}{V_n}\right)}\right] \quad \text{(Eq. 1)}$$

where F_0 is the initial nuclear fluorescence, F_{max} is the maximal nuclear fluorescence reached, $t_{½}$ is the time (min) at which fluorescence is halfway between F_0 and F_{max}, and V_n is a factor determining how steeply nuclear accumulation changes with time.

Analysis of MR Transactivation Function

Different proportions of WT and mutant MR were co-transfected with a plasmid containing firefly luciferase under the control of a synthetic promoter with two copies of the glucocorticoid/mineralocorticoid-responsive element (GRE2X; kindly provided by Dr. Rainer Lanz, Baylor College of Medicine, Houston, TX). Transfection efficiency was controlled by co-transfection of a plasmid encoding *Renilla* luciferase under a cytomegalovirus promoter (pSG5-ren, kindly provided by Dr. Fátima Gebauer, Center for Genomic Regulation, Barcelona, Spain). Firefly and *Renilla* luciferase activities were measured sequentially in cell lysates using a commercial kit (Dual-Glo; Promega, Madison, WI). EC_{50} values were calculated from normalized data fitted to a log(agonist) *versus* response equation with variable slope using Prism 5.

Analysis of MR Dimerization and Interaction with Co-regulators by in Situ PLA

PLA was performed using a commercially available kit (Duolink, Olink Biosciences, Uppsala, Sweden) as recently described (26). To assess interaction of MR with co-regulators, COS-7 cells were transfected with MR-147-YFP and pcDNA3.1-SRC-1-HA. To study MR dimerization, MR-147-HA was co-transfected with MR-147-YFP or MR-147-YFP-S839D. The antibodies used in these assays were rabbit polyclonal anti-GFP antibody (a kind gift from Dr. Raimundo Freire) and mouse monoclonal anti-HA antibody (clone HA.11, Covance, Madrid, Spain) and were validated by immunocytochemistry using previously described procedures (5, 7). Negative controls consisted on omitting one of the transfected plasmids. When indicated, cells were treated with 10 nM aldosterone overnight. Results were quantified using the software provided by the manufacturer (Duolink Image Tool) and are expressed as average number of puncta/cell area.

Structure Modeling and Ligand Docking

General—All calculations were performed on a Windows 7 PC with six core Intel i7–4930K processor (3.4GHz) with 16 gigabytes total RAM using Schrödinger's Biologics and Small-Molecule Drug Discovery suites of software programs (Schrödinger, LLC, New York).

Ligand Preparation—LigPrep was used to produce low energy three-dimensional conformations of all docked compounds, and Epik was used to generate their ionization/tautomeric states. The chiralities of the compounds were retained from the original state, and ligands conformations were minimized using OPLS-2005 force field.

Protein Preparation—The receptor ligand binding domain crystallographic structure was loaded from the Protein Data Bank (PDB) and prepared by using Protein Preparation Wizard. We used the structure with the PDB ID 3VHU (12). We assigned bond orders, added missing H atoms, and filled in the missing loops and the side chains using Prime. Water molecules beyond 5 Å from co-crystallized ligand were deleted, and ionization/tautomeric states were generated at pH 7.0 ± 2.0 using Epik. Afterward, the protein structures were refined by optimizing hydrogen bonds (H-bonds) and sampling water molecules orientations. At the end, a restrained minimization (<0.30 Å for each heavy atom) was performed using OPLS-2005 force field.

Ligand Docking—All the docking calculations were performed with Glide SP algorithm with the final scoring using the GlideScore. Docking grids were generated by Glide using the co-crystallized ligand at the center of the grid box. The compounds were docked flexibly, and after docking we kept the 20 best docked conformations for each pair ligand/receptor.

Receptor Modeling—Receptor variants of interest (the phosphomimetic and the phosphorylated ones) were generated using BioLuminate, which uses a rotamer library in Prime for side-chain sampling with a variable dielectric treatment of polarization from the protein side chains and an implicit solvent surface generalized born model with the OPLS-2005 force field for energy evaluations. The receptor variants were generated by sampling and refining all residues side chain and backbone atoms within 5 Å of the mutated residues using Prime side-chain prediction combined with backbone sampling.

Author Contributions—R. J.-C. conducted most of the experiments. R. J.-C. and D. A. R. analyzed the results and wrote most of the paper. M. X. F. conducted *in silico* simulations and contributed to analyzing and interpreting data and writing of the paper. D. A. R. conceived the idea for the project. All authors corrected and approved the final version of the manuscript.

Acknowledgments—We thank Dr. Nicolette Farman, Dr. Raimundo Freire, Dr. Fátima Gebauer, and Dr. Rainer Lanz for the kind gift of reagents.

References

1. Sever, R., and Glass, C. K. (2013) Signaling by nuclear receptors. *Cold Spring Harb. Perspect. Biol.* **5,** a016709
2. McKenna, N. J., and O'Malley, B. W. (2002) Combinatorial control of gene expression by nuclear receptors and coregulators. *Cell* **108,** 465–474
3. Anbalagan, M., Huderson, B., Murphy, L., and Rowan, B. G. (2012) Post-translational modifications of nuclear receptors and human disease. *Nucl. Recept. Signal.* **10,** e001
4. Shibata, S., Rinehart, J., Zhang, J., Moeckel, G., Castañeda-Bueno, M., Stiegler, A. L., Boggon, T. J., Gamba, G., and Lifton, R. P. (2013) Mineralocorticoid receptor phosphorylation regulates ligand binding and renal response to volume depletion and hyperkalemia. *Cell Metab.* **18,** 660–671
5. Aguilar-Sánchez, C., Hernández-Díaz, I., Lorenzo-Díaz, F., Navarro, J. F., Hughes, T. E., Giraldez, T., and Alvarez de la Rosa, D. (2012) Identification of permissive insertion sites for generating functional fluorescent mineralocorticoid receptors. *Endocrinology* **153,** 3517–3525
6. Farman, N., and Rafestin-Oblin, M. E. (2001) Multiple aspects of mineralocorticoid selectivity. *Am. J. Physiol. Renal Physiol.* **280,** F181–F192
7. Hernández-Díaz, I., Giraldez, T., Arnau, M. R., Smits, V. A., Jaisser, F., Farman, N., and Alvarez de la Rosa, D. (2010) The mineralocorticoid receptor is a constitutive nuclear factor in cardiomyocytes due to hyperactive nuclear localization signals. *Endocrinology* **151,** 3888–3899
8. Walther, R. F., Atlas, E., Carrigan, A., Rouleau, Y., Edgecombe, A., Visentin, L., Lamprecht, C., Addicks, G. C., Haché, R. J., and Lefebvre, Y. A. (2005) A serine/threonine-rich motif is one of three nuclear localization signals that determine unidirectional transport of the mineralocorticoid receptor to the nucleus. *J. Biol. Chem.* **280,** 17549–17561
9. Amazit, L., Le Billan, F., Kolkhof, P., Lamribet, K., Viengchareun, S., Fay, M. R., Khan, J. A., Hillisch, A., Lombès, M., Rafestin-Oblin, M. E., and Fagart, J. (2015) Finerenone impedes aldosterone-dependent nuclear import of the mineralocorticoid receptor and prevents genomic recruitment of steroid receptor coactivator-1. *J. Biol. Chem.* **290,** 21876–21889
10. Hultman, M. L., Krasnoperova, N. V., Li, S., Du, S., Xia, C., Dietz, J. D., Lala, D. S., Welsch, D. J., and Hu, X. (2005) The ligand-dependent interaction of mineralocorticoid receptor with coactivator and corepressor peptides suggests multiple activation mechanisms. *Mol. Endocrinol.* **19,** 1460–1473
11. Li, Y., Suino, K., Daugherty, J., and Xu, H. E. (2005) Structural and biochemical mechanisms for the specificity of hormone binding and coactivator assembly by mineralocorticoid receptor. *Mol. Cell* **19,** 367–380
12. Hasui, T., Matsunaga, N., Ora, T., Ohyabu, N., Nishigaki, N., Imura, Y., Igata, Y., Matsui, H., Motoyaji, T., Tanaka, T., Habuka, N., Sogabe, S., Ono, M., Siedem, C. S., Tang, T. P., Gauthier, C., De Meese, L. A., Boyd, S. A., and Fukumoto, S. (2011) Identification of benzoxazin-3-one derivatives as novel, potent, and selective nonsteroidal mineralocorticoid receptor antagonists. *J. Med. Chem.* **54,** 8616–8631
13. Funder, J. W. (2013) Angiotensin retains sodium by dephosphorylating mineralocorticoid receptors in renal intercalated cells. *Cell Metab.* **18,** 609–610
14. Liu, W., Wang, J., Sauter, N. K., and Pearce, D. (1995) Steroid receptor heterodimerization demonstrated in vitro and in vivo. *Proc. Natl. Acad. Sci. U.S.A.* **92,** 12480–12484
15. Hellal-Levy, C., Couette, B., Fagart, J., Souque, A., Gomez-Sanchez, C., and Rafestin-Oblin, M. (1999) Specific hydroxylations determine selective corticosteroid recognition by human glucocorticoid and mineralocorticoid receptors. *FEBS Lett.* **464,** 9–13
16. Hellal-Levy, C., Fagart, J., Souque, A., and Rafestin-Oblin, M. E. (2000) Mechanistic aspects of mineralocorticoid receptor activation. *Kidney Int.* **57,** 1250–1255
17. Lombes, M., Kenouch, S., Souque, A., Farman, N., and Rafestin-Oblin, M. E. (1994) The mineralocorticoid receptor discriminates aldosterone from glucocorticoids independently of the 11 β-hydroxysteroid dehydrogenase. *Endocrinology* **135,** 834–840
18. Kino, T., Jaffe, H., Amin, N. D., Chakrabarti, M., Zheng, Y. L., Chrousos, G. P., and Pant, H. C. (2010) Cyclin-dependent kinase 5 modulates the transcriptional activity of the mineralocorticoid receptor and regulates expression of brain-derived neurotrophic factor. *Mol. Endocrinol.* **24,** 941–952
19. Mani, O., Nashev, L. G., Livelo, C., Baker, M. E., and Odermatt, A. (2016) Role of Pro-637 and Gln-642 in human glucocorticoid receptors and Ser-843 and Leu-848 in mineralocorticoid receptors in their differential responses to cortisol and aldosterone. *J. Steroid. Biochem. Mol. Biol.* **159,** 31–40
20. Moras, D., and Gronemeyer, H. (1998) The nuclear receptor ligand-binding domain: structure and function. *Curr. Opin. Cell Biol.* **10,** 384–391
21. Gravez, B., Tarjus, A., Jimenez-Canino, R., El Moghrabi, S., Messaoudi, S., Alvarez de la Rosa, D., and Jaisser, F. (2013) The diuretic torasemide does not prevent aldosterone-mediated mineralocorticoid receptor activation in cardiomyocytes. *PloS ONE* **8,** e73737
22. Ou, X. M., Storring, J. M., Kushwaha, N., and Albert, P. R. (2001) Heterodimerization of mineralocorticoid and glucocorticoid receptors at a novel negative response element of the 5-HT1A receptor gene. *J. Biol. Chem.* **276,** 14299–14307
23. Gomez-Sanchez, C. E., de Rodriguez, A. F., Romero, D. G., Estess, J., Warden, M. P., Gomez-Sanchez, M. T., and Gomez-Sanchez, E. P. (2006) Development of a panel of monoclonal antibodies against the mineralocorticoid receptor. *Endocrinology* **147,** 1343–1348
24. Refolio, E., Cavero, S., Marcon, E., Freire, R., and San-Segundo, P. A. (2011) The Ddc2/ATRIP checkpoint protein monitors meiotic recombination intermediates. *J. Cell Sci.* **124,** 2488–2500
25. Cheng, Y., and Prusoff, W. H. (1973) Relationship between the inhibition constant (K1) and the concentration of inhibitor which causes 50 percent inhibition (I_{50}) of an enzymatic reaction. *Biochem. Pharmacol.* **22,** 3099–3108
26. Jiménez-Canino, R., Lorenzo-Díaz, F., Jaisser, F., Farman, N., Giraldez, T., and Alvarez de la Rosa, D. (2016) Histone deacetylase 6-controlled Hsp90 acetylation significantly alters mineralocorticoid receptor subcellular dynamics but not its transcriptional activity. *Endocrinology* **157,** 2515–2532